



Cite this: *RSC Adv.*, 2020, **10**, 42354

## Visible-light-driven $\text{CO}_2$ reduction to formate with a system of water-soluble zinc porphyrin and formate dehydrogenase in ionic liquid/aqueous media

Francesco Secundo <sup>a</sup> and Yutaka Amao <sup>\*bc</sup>

Visible-light-driven  $\text{CO}_2$  reduction to formate with a system consisting of water-soluble zinc tetraphenylporphyrin tetrasulfonate (ZnTPPS), formate dehydrogenase from *Candida boidinii* (CbFDH) and methylviologen (MV) in the presence of triethanolamine (TEOA) as an electron donor in an ionic liquid, 1-ethyl-3-methylimidazolium dimethyl phosphate ( $[\text{EMIm}][\text{Me}_2\text{PO}_4]$ )/aqueous media was investigated. The catalytic activity of CbFDH for formate oxidation to  $\text{CO}_2$  and  $\text{CO}_2$  reduction to formate did not decrease significantly even in  $[\text{EMIm}][\text{Me}_2\text{PO}_4]$ /aqueous media, compared with that in aqueous media. The visible-light-driven MV reduction by the photosensitization of ZnTPPS in  $[\text{EMIm}][\text{Me}_2\text{PO}_4]$ /aqueous media proceeds more efficiently than in the aqueous media system. In the visible-light-driven  $\text{CO}_2$  reduction to formate system of ZnTPPS, MV and CbFDH with  $[\text{EMIm}][\text{Me}_2\text{PO}_4]$ /aqueous media, moreover, the formate production concentration after 180 min decreased by only 20% as compared with the system in aqueous media.

Received 9th October 2020  
 Accepted 9th November 2020

DOI: 10.1039/d0ra08594d  
[rsc.li/rsc-advances](http://rsc.li/rsc-advances)

## Introduction

Climate change is a problem primarily caused by the surge in  $\text{CO}_2$  in the atmosphere.<sup>1</sup> As one of the solutions to these problems, solar energy-based  $\text{CO}_2$  utilization technologies have received considerable attention. Among these technologies, a system of light-driven  $\text{CO}_2$  reduction to CO, formate or methanol, consisting of a photosensitizer, an electron mediator and a biocatalyst, was developed.<sup>2–14</sup> Among these biocatalysts, formate dehydrogenase (FDH) catalyzes the  $\text{CO}_2$  reduction to formate in the presence of a co-enzyme such as NADH, and single-electron reduced 4,4'- or 2,2'-bipyridinium salts (BP). Thus, visible-light-driven  $\text{CO}_2$  reduction to formate system is developed with the photoredox system of a photosensitizer, an electron mediator and FDH. NAD<sup>+</sup>-dependent FDH derived from *Candida boidinii* (CbFDH) is commercially available biocatalyst and is widely utilized in the visible-light-driven redox system for  $\text{CO}_2$  reduction to formate.<sup>5,9–14</sup> NAD<sup>+</sup>-dependent FDHs catalyze the formate oxidation to  $\text{CO}_2$  with the co-enzyme NAD<sup>+</sup> and catalyze the  $\text{CO}_2$  reduction to formate with NADH, as shown in Fig. 1.

Visible-light-driven  $\text{CO}_2$  reduction to formate with CbFDH and methylviologen (MV) reduction with a system containing ruthenium(II) coordination compound as a photosensitizer and mercaptoethanol as an electron donor has been reported for the first time.<sup>5</sup> In contrast, we previously reported the visible-light-driven  $\text{CO}_2$  reduction to formate with the system consisting of MV, CbFDH and water-soluble zinc porphyrin (zinc tetraphenylporphyrin tetrasulfonate; ZnTPPS or zinc 5,10,15,20-tetrakis(1-methyl-4-pyridinio)porphyrin; ZnTMPyP)<sup>10</sup> or chlorophyll-a<sup>13</sup> in the presence of triethanolamine (TEOA) as an electron donor as shown in Fig. 2.

We also previously reported the visible-light-driven  $\text{CO}_2$  reduction to formate with the system consisting of various 2,2'<sup>11</sup> or 4,4'-BPs,<sup>12,14</sup> CbFDH and water-soluble zinc porphyrin. NAD<sup>+</sup> cannot be directly reduced to NADH in the photoredox system using ZnTPPS or ruthenium(II) coordination compounds. Instead, 2,2'- or 4,4'-BPs can be easily reduced to cation radical of BPs by the photoredox system using these photosensitizers. The cation radical of BP acts as a co-enzyme for CbFDH-catalyzed  $\text{CO}_2$  reduction to formate.<sup>15,16</sup>

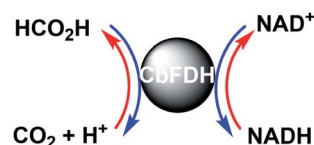


Fig. 1 Interconversion between formate and  $\text{CO}_2$  catalyzed with FDH using natural co-enzyme NAD<sup>+</sup>/NADH redox coupling.

<sup>a</sup>*Istituto di Scienze e Tecnologie Chimiche “Giulio Natta”, CNR Via Mario Bianco 9, 20131 Milano, Italy*

<sup>b</sup>*Graduate School of Science, Osaka City University, 3-3-138 Sugimoto, Sumiyoshi-ku, Osaka 558-8585, Japan*

<sup>c</sup>*Research Centre of Artificial Photosynthesis (ReCAP), Osaka City University, 3-3-138 Sugimoto, Sumiyoshi-ku, Osaka 558-8585, Japan. E-mail: [amao@osaka-cu.ac.jp](mailto:amao@osaka-cu.ac.jp)*



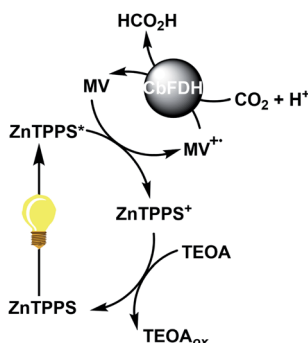


Fig. 2 Visible-light-driven  $\text{CO}_2$  reduction to formate with the photoredox system consisting of TEOA as an electron donor, ZnTPPS as a photosensitizer, MV as an electron mediator and CbFDH.

The  $\text{CO}_2$  utilization technology is expected to be used not only for solving environmental problems but also for specific environments where temperatures are extremely low. For example, NASA's  $\text{CO}_2$  Conversion Challenge,<sup>17</sup> a Centennial Challenges competition, seeks to incentivize the public to develop non-biological systems that can convert  $\text{CO}_2$  into useful sugar molecules in Mars. The previously reported visible-light-driven  $\text{CO}_2$  reduction system is not applicable in the specific environment of Mars, where  $\text{CO}_2$  occupies more than 90% of the atmosphere, the average temperature is  $-53^\circ\text{C}$ , and the atmospheric pressure is 0.9 kPa. Therefore, the need to construct a visible-light-driven  $\text{CO}_2$  reduction system below the freezing point of water is expected shortly. One of the means for solving these problems is to use an ionic liquid as a reaction medium. An ionic liquid is a salt in the liquid state.<sup>18-27</sup> There are ionic liquids that remain liquid at low pressures close to vacuum and below  $-50^\circ\text{C}$ . For example, ionic liquids that are liquid below  $-143^\circ\text{C}$  have been proposed as the fluid base for a spinning liquid-mirror telescope to be based on the Moon.<sup>28</sup> By dissolving frozen water molecules in an ionic liquid, thus, it might be a prerequisite for a light-driven  $\text{CO}_2$  reduction system. There have been numerous reports on biocatalytic reactions using ionic liquids or ionic liquids/water as a medium.<sup>29-36</sup> Several studies on the enzymatic activity of FDH in ionic liquids have also been reported.<sup>37,38</sup> So far, there have been no reports on ionic liquids or ionic liquids/water-based light-driven  $\text{CO}_2$  reduction system of an electron donor, a photosensitizer, an electron mediator, and biocatalyst. In other words, since a normal buffer solution cannot be used in an extreme environment, it is necessary to use it as a solvent for an ionic liquid. As the first step to achieve the visible-light-driven  $\text{CO}_2$  reduction to formate with the system of a photosensitizer and CbFDH in the extreme environment, whether or not an efficient reaction system in the ionic liquids or ionic liquids/water can be constructed is an important key point.

In this article, to enable the construction of the visible-light-driven  $\text{CO}_2$  reduction to formate with the system of a photosensitizer and CbFDH in ionic liquid/aqueous media, CbFDH-catalyzed formate oxidation and  $\text{CO}_2$  reduction are investigated in ionic liquid, 1-ethyl-3-methylimidazolium dimethyl phosphate ([EMIm]  $[\text{Me}_2\text{PO}_4]$ ; chemical structure as shown in Fig. 3) and aqueous

media. Finally, the visible-light-driven  $\text{CO}_2$  reduction to formate with the system consisting of ZnTPPS, MV and CbFDH in the [EMIm]  $[\text{Me}_2\text{PO}_4]$ /aqueous media were studied.

## Experimental

### Materials

FDH from *Candida boidinii* (CbFDH) was purchased from Roche Diagnostics K.K. The estimated molecular weight of CbFDH was reported to be 74 kDa.<sup>39</sup> Tetraphenylporphyrin tetrasulfonate (H<sub>2</sub>TPPS), TEOA, and MV were supplied by Tokyo Kasei Co. Ltd. NAD<sup>+</sup> and NADH were supplied by Oriental Yeast Co., Ltd. 1-Ethyl-3-methylimidazolium dimethyl phosphate ([EMIm]  $[\text{Me}_2\text{PO}_4]$ ) was purchased from Sigma-Aldrich Co. LLC. The other chemicals were of analytical grade or the highest grade available purchased from Wako Pure Chemical Co., Ltd. ZnTPPS was prepared by refluxing H<sub>2</sub>TPPS with about 10 times molar equivalent of zinc acetate according to previously reported literature.<sup>40-43</sup> The removal of the small amount of zinc acetate from the prepared ZnTPPS solution was omitted because zinc acetate does not influence the following photoreactions.<sup>40-43</sup> The stability of ZnTPPS against continuous visible-light irradiation was also checked.

### Enzymatic activity test of CbFDH in the ionic liquid/aqueous media

The catalytic activity of CbFDH in the ionic liquid/water media was studied by monitoring the formate oxidation to  $\text{CO}_2$  as follows. The sample solution consisted of sodium formate (16 mM), CbFDH (9.2  $\mu\text{M}$ ) and NAD<sup>+</sup> (200  $\mu\text{M}$ ) in 30% w/w [EMIm]  $[\text{Me}_2\text{PO}_4]$  containing 50 mM sodium pyrophosphate buffer (pH 7.4) saturated with nitrogen gas. The absorption of the NADH was detected at 340 nm ( $\varepsilon_{340} = 6300 \text{ M}^{-1} \text{ cm}^{-1}$ )<sup>44</sup> using UV-visible absorption spectroscopy (SHIMADZU, MultiSpec-1500).

To study the  $\text{CO}_2$  reduction catalyst activity with CbFDH in the ionic liquid/water media, the  $\text{CO}_2$  reduction to formate was carried out as follows. The sample solution consisted of NADH (160  $\mu\text{M}$ ) and CbFDH (9.2  $\mu\text{M}$ ) in 30% w/w [EMIm]  $[\text{Me}_2\text{PO}_4]$  containing 50 mM sodium pyrophosphate buffer (pH 7.4) saturated with  $\text{CO}_2$  gas. The total concentration of carbonate species ( $\text{CO}_2$  and  $\text{HCO}_3^-$ ) in the  $\text{CO}_2$  saturated sodium pyrophosphate buffer (pH 7.4) was estimated to be approximately 74 mM. As the abundance ratio of  $\text{CO}_2$  to  $\text{HCO}_3^-$  ( $[\text{CO}_2]/[\text{HCO}_3^-]$ ) was estimated to be 0.064 at pH 7.4 buffer solution under atmospheric pressure,<sup>45-47</sup> the concentration of  $\text{CO}_2$  in

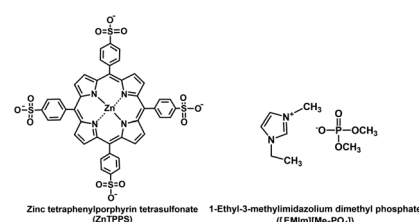


Fig. 3 Chemical structures of ZnTPPS and 1-ethyl-3-methylimidazolium dimethyl phosphate ([EMIm]  $[\text{Me}_2\text{PO}_4]$ ).



sodium pyrophosphate buffer (pH 7.4) was estimated to be 4.4 mM. The absorption of the NADH was detected at 340 nm using UV-visible absorption spectroscopy (SHIMADZU, MultiSpec-1500).

### Electrochemical measurements of MV in the ionic liquid/aqueous media

The single and double-electron reduction potentials for MV in the ionic liquid/water media was determined by cyclic voltammetry (Hokuto Denko HZ-3000). All measurements were carried out under 2.0 mM of MV in nitrogen-saturated solution containing 30% w/w [EMIm][Me<sub>2</sub>PO<sub>4</sub>], 0.2 M potassium chloride and 1.0 mM sodium pyrophosphate buffer (pH 7.4) at a glassy carbon-working electrode. A platinum wire was used as a counter electrode. All potentials were relative to the Ag/AgCl electrode used as the reference.

### Visible-light-driven MV reduction with photosensitization of ZnTPPS in the ionic liquid/aqueous media

A solution consisting of TEOA (0.3 M), ZnTPPS (10  $\mu$ M) and MV (100  $\mu$ M) in 30% w/w [EMIm][Me<sub>2</sub>PO<sub>4</sub>] containing 5.0 ml of 10 mM sodium pyrophosphate buffer (pH 7.4) was deaerated by Ar gas bubbling for 30 min. The sample solution was irradiated with a 250 W halogen lamp (TOSHIBA JD110V215WNP-EH-TB) at a distance of 5.0 cm at 30 °C. The experiment was carried out in a water-bath made by polymethyl methacrylate (PMMA), and light shorter than the wavelength of 365 nm of the halogen lamp was cut off by PMMA. The production of the MV<sup>+</sup> was monitored by UV-vis absorption spectrum.

### Visible-light-driven CO<sub>2</sub> reduction to formate with the system consisting of ZnTPPS, MV and CbFDH in the ionic liquid/aqueous media

A solution consisting of TEOA (0.3 M), ZnTPPS (10  $\mu$ M), MV (100  $\mu$ M) and CbFDH (9.2  $\mu$ M) in 30% w/w [EMIm][Me<sub>2</sub>PO<sub>4</sub>] containing 5.0 ml of 10 mM sodium pyrophosphate buffer (pH 7.4) was deaerated by freeze-pump-thaw cycles repeated 5 times, and the gas phase was replaced with CO<sub>2</sub>. The sample solution was irradiated with a 250 W halogen lamp at 30 °C. The experiment also was carried out in a water-bath made by PMMA, and light shorter than the wavelength of 365 nm of the halogen lamp was cut off by PMMA. The amount of formate was detected by ion chromatography (Dionex ICS-1100; electrical conductivity detector) with an ion exclusion column (Thermo ICE AS1; column length: 9 × 150 mm; composed of a 7.5  $\mu$ m cross-linked styrene/divinylbenzene resin with functionalized sulfonate groups). The 1.0 mM octane sulfonic acid and 5.0 mM tetrabutylammonium hydroxide were used as an eluent and a regenerant, respectively.

## Results and discussion

### Enzymatic activity test of CbFDH in the ionic liquid/aqueous media

When the sample solution of sodium formate (16 mM), CbFDH (9.2  $\mu$ M) and NAD<sup>+</sup> (200  $\mu$ M) in 30% w/w [EMIm][Me<sub>2</sub>PO<sub>4</sub>]

containing 50 mM sodium pyrophosphate buffer (pH 7.4) was incubated, absorption spectra of the solution were changed as shown in Fig. 4. The absorption band at 340 nm due to NADH was increased with increasing incubation time.

From the result of Fig. 4, it was shown that CbFDH-catalyzed NAD<sup>+</sup> reduction to NADH, that is, formate oxidation to CO<sub>2</sub>, proceeded in the ionic liquid/aqueous media. It was suggested that CbFDH-catalyzed oxidation of formate to CO<sub>2</sub> proceeds in an ionic liquid/aqueous medium.

When the sample solution of CbFDH (9.2  $\mu$ M) and NADH (160  $\mu$ M) in 30% w/w [EMIm][Me<sub>2</sub>PO<sub>4</sub>] containing CO<sub>2</sub> saturated 50 mM sodium pyrophosphate buffer (pH 7.4) was incubated, absorption spectra of the solution were changed as shown in Fig. 5. The absorption band at 340 nm due to NADH was decreased with increasing incubation time.

From the result of Fig. 5, it is shown NADH oxidation to NAD<sup>+</sup>, which indicates that the CbFDH-catalyzed reduction of CO<sub>2</sub> to formate also proceeds in an ionic liquid/aqueous medium.

Next, let us focus on the effect of [EMIm][Me<sub>2</sub>PO<sub>4</sub>] on the CbFDH-catalyzed oxidation of formate to CO<sub>2</sub> and reduction of CO<sub>2</sub> to formate using NAD<sup>+</sup>/NADH redox mediator. Fig. 6 shows the time dependence of NADH concentration changes of CbFDH-catalyzed oxidation of formate to CO<sub>2</sub> (a) and reduction of CO<sub>2</sub> to formate (b) in the [EMIm][Me<sub>2</sub>PO<sub>4</sub>]/aqueous or aqueous media.

For the CbFDH-catalyzed oxidation of formate to CO<sub>2</sub> in aqueous media, NAD<sup>+</sup> fully was reduced to NADH within 20 min incubation. For the system in the [EMIm][Me<sub>2</sub>PO<sub>4</sub>]/aqueous media, in contrast, the conversion yield of NAD<sup>+</sup> to NADH was estimated to be 50% for 140 min incubation. The Michaelis constant  $K_m$  values of NAD<sup>+</sup> for CbFDH-catalyzed formate oxidation to CO<sub>2</sub> in aqueous and [EMIm][Me<sub>2</sub>PO<sub>4</sub>]/aqueous media obtained by using enzymatic kinetic analysis were reported to be 43 and 177  $\mu$ M, respectively.<sup>37</sup> In other words, it was suggested that the affinity of NAD<sup>+</sup> for CbFDH in the [EMIm][Me<sub>2</sub>PO<sub>4</sub>]/aqueous media was lower than that in the aqueous media. Therefore, it was considered that the conversion yield of NAD<sup>+</sup> to NADH in [EMIm][Me<sub>2</sub>PO<sub>4</sub>]/aqueous media was lower than that in aqueous media.

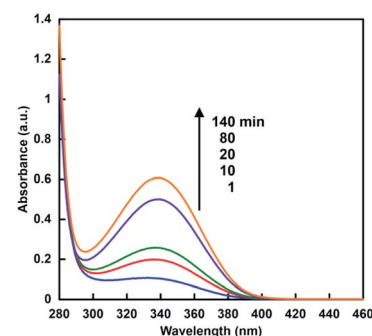


Fig. 4 UV-vis absorption spectra changes in the solution of sodium formate (16 mM), CbFDH (9.2  $\mu$ M) and NAD<sup>+</sup> (200  $\mu$ M) in 30% w/w [EMIm][Me<sub>2</sub>PO<sub>4</sub>] containing 50 mM sodium pyrophosphate buffer (pH 7.4) with incubation time.



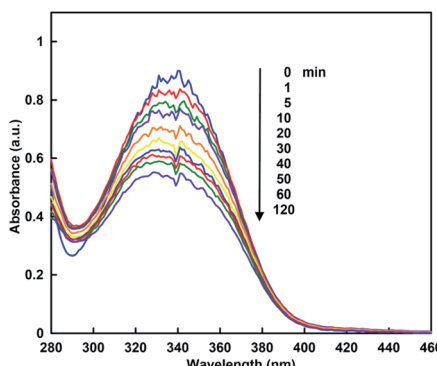


Fig. 5 UV-vis absorption spectra changes in the solution of CbFDH (9.2  $\mu$ M) and NADH (160  $\mu$ M) in 30 w/w% [EMIm][Me<sub>2</sub>PO<sub>4</sub>] containing CO<sub>2</sub> saturated 50 mM sodium pyrophosphate buffer (pH 7.4) with incubation time.

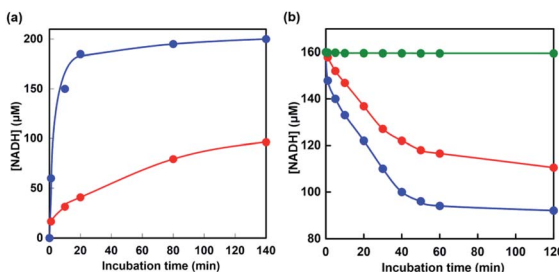


Fig. 6 Time dependence of NADH concentration changes of CbFDH-catalyzed oxidation of formate to CO<sub>2</sub> (a) and reduction of CO<sub>2</sub> to formate (b) in the [EMIm][Me<sub>2</sub>PO<sub>4</sub>]/aqueous (red) or aqueous media (blue). Green: time dependence of NADH concentration changes in Ar-saturated NADH solution in [EMIm][Me<sub>2</sub>PO<sub>4</sub>]/aqueous containing CbFDH in (b).

For the CbFDH-catalyzed reduction of CO<sub>2</sub> to formate in aqueous media, the conversion yield of NADH to NAD<sup>+</sup> was estimated to be 40% after 120 min incubation. For the system in the [EMIm][Me<sub>2</sub>PO<sub>4</sub>]/aqueous media, in contrast, the conversion yield was estimated to be 30% after 120 min incubation. Moreover, after 120 min of incubation, 200 mM sodium formate was added to this solution and NADH production was observed again. This suggests that the catalytic activity of CbFDH is not inactivated in the [EMIm][Me<sub>2</sub>PO<sub>4</sub>]/aqueous media. On the other hand, in an Ar-saturated [EMIm][Me<sub>2</sub>PO<sub>4</sub>]/aqueous media, that is, in the absence of CO<sub>2</sub>, the concentration of NADH has dropped by only 0.33% over the 120 min. From these results, the decrease in NADH, as shown in Fig. 6(b), is due to CbFDH-catalyzed CO<sub>2</sub> reduction to formate rather than air oxidation of NADH to NAD<sup>+</sup>. In aqueous media and [EMIm][Me<sub>2</sub>PO<sub>4</sub>]/aqueous media, the CbFDH-catalyzed formate oxidation to CO<sub>2</sub> proceeded more efficiently than the CO<sub>2</sub> reduction to formate. We determined the kinetic parameters for the Michaelis constants ( $K_m$ ) of NAD<sup>+</sup> and NADH for CbFDH in the formate oxidation to CO<sub>2</sub> and in the reverse reaction under the condition of an excess of formate or CO<sub>2</sub>. The  $K_m$  values for NAD<sup>+</sup> in the formate oxidation and NADH in the CO<sub>2</sub> reduction

to CbFDH were estimated to be 50 and 2087  $\mu$ M, respectively. Thus, being the affinity of NAD<sup>+</sup> for CbFDH higher than that of NADH, CbFDH can be activated by a lower concentration of NAD<sup>+</sup>, compared with that of NADH (1/400).<sup>48,49</sup> The CbFDH-catalyzed oxidation of formate to CO<sub>2</sub> and reduction of CO<sub>2</sub> to formate was slower in the [EMIm][Me<sub>2</sub>PO<sub>4</sub>]/aqueous media than in the aqueous media. However, these results indicate that the catalytic activity of CbFDH is not inactivated even in the [EMIm][Me<sub>2</sub>PO<sub>4</sub>]/aqueous media.

### Electrochemical property of MV in the ionic liquid/water media

Fig. 7 shows the cyclic voltammogram (CV) of MV in the nitrogen-saturated solution containing 30% w/w [EMIm][Me<sub>2</sub>PO<sub>4</sub>], 0.2 M potassium chloride and 1.0 mM sodium pyrophosphate buffer (pH 7.4). The CV of MV in the nitrogen-saturated solution containing 0.2 M potassium chloride and 1.0 mM sodium pyrophosphate buffer (pH 7.4) also was shown in Fig. 7.

The reduction potentials for single and double-electron reduced MV (vs. Ag/AgCl) were estimated to be  $-0.66$  and  $-0.96$  V in aqueous media, respectively. In contrast, the reduction potentials for single and double-electron reduced MV (vs. Ag/AgCl) were estimated to be  $-0.68$  and  $-0.96$  V in [EMIm][Me<sub>2</sub>PO<sub>4</sub>]/aqueous media, respectively. The first reduction potential difference of MV between the [EMIm][Me<sub>2</sub>PO<sub>4</sub>]/aqueous and the aqueous media was estimated to be only 20 mV. As a result of cyclic voltammetry measurement, thus, it was concluded that there was almost no difference between the [EMIm][Me<sub>2</sub>PO<sub>4</sub>]/aqueous and aqueous media.

### Visible-light-driven MV reduction with photosensitization of ZnTPPS in the ionic liquid/aqueous media

When the solution consisting of TEOA, ZnTPPS and MV in 30% w/w [EMIm][Me<sub>2</sub>PO<sub>4</sub>] containing 5.0 ml of 10 mM sodium pyrophosphate buffer (pH 7.4) was irradiated with visible-light, the absorption spectra of the solution were changed with irradiation time. Fig. 8 shows the absorption difference spectra change with the solution as a baseline before irradiation. The absorption band at 605 nm due to MV<sup>+</sup> was increased with

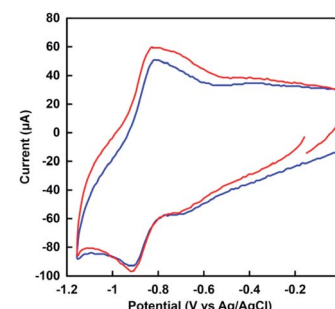


Fig. 7 Cyclic voltammogram of MV (2.0 mM) in nitrogen-saturated sodium pyrophosphate buffer (pH 7.4) containing 30% w/w [EMIm][Me<sub>2</sub>PO<sub>4</sub>] and 0.2 M potassium chloride (red). Blue: in the absence of [EMIm][Me<sub>2</sub>PO<sub>4</sub>].



increasing irradiation time. Thus, the single-electron reduction of MV proceeded with the visible-light sensitization of ZnTPPS in the  $[\text{EMIm}][\text{Me}_2\text{PO}_4]$ /aqueous media.

The time dependence of the concentration changes of  $\text{MV}^{+*}$  produced was determined by molar coefficient with  $13\,500\, \text{M}^{-1}\, \text{cm}^{-1}$  at  $605\, \text{nm}$ .<sup>50</sup> Fig. 9 shows the relationship between the irradiation time and the concentration of  $\text{MV}^{+*}$  in the  $[\text{EMIm}][\text{Me}_2\text{PO}_4]$ /aqueous (red) or aqueous media (blue).

The amount of  $\text{MV}^{+*}$  increased with increasing irradiation time in both cases. The initial rate was determined from the gradient of the linear part of the  $\text{MV}^{+*}$  production within 5 min irradiation. The initial rates for the  $\text{MV}^{+*}$  production in  $[\text{EMIm}][\text{Me}_2\text{PO}_4]$ /aqueous and aqueous media were estimated to be  $4.7$  and  $2.7\, \mu\text{M}\, \text{min}^{-1}$ , respectively. After 30 min irradiation, the concentrations of  $\text{MV}^{+*}$  in  $[\text{EMIm}][\text{Me}_2\text{PO}_4]$ /aqueous and aqueous media were estimated to be  $46.8$  and  $33.0\, \mu\text{M}$ , respectively. The results for the visible-light-driven reduction of MV with the sensitization of ZnTPPS in  $[\text{EMIm}][\text{Me}_2\text{PO}_4]$ /aqueous media and aqueous media were summarized in Table 1.

Regarding the electron transfer pathway from photoexcited state of ZnTPPS to MV, the mechanism of the electron transfer process from the excited triplet state of ZnTPPS ( ${}^3\text{ZnTPPS}^*$ ) to MV has been reported using nano-second order laser flash photolysis.<sup>51</sup> The oxidation potential for TEOA was reported to be  $0.93\, \text{V}$  (vs. Ag/AgCl).<sup>52</sup> The energy level of first singlet state for ZnTPPS was estimated to be  $2.07\, \text{eV}$  using the average value of the frequencies of the longest wavelength of the absorption maxima ( $595\, \text{nm}$ ) and the shortest wavelength of the fluorescence emission maxima ( $606\, \text{nm}$ ). The potential for the single-electron oxidation of the  ${}^3\text{ZnTPPS}^*$ ,  $E(\text{ZnTPPS}^+/{^3\text{ZnTPPS}^*})$  was estimated to be  $-0.75\, \text{V}$  (vs. Ag/AgCl).<sup>53,54</sup> On the other hand, the potential for the single-electron reduction of  ${}^3\text{ZnTPPS}^*$ ,  $E({^3\text{ZnTPPS}^*}/\text{ZnTPPS}^-)$  was reported to be  $0.45\, \text{V}$  (vs. Ag/AgCl).<sup>53</sup> According to these potentials, it was shown that no single-electron reduction of  ${}^3\text{ZnTPPS}^*$  by TEOA proceeded. That is,  ${}^3\text{ZnTPPS}^*$  is not reductively quenched by TEOA. The single-electron reduction potentials for MV in  $[\text{EMIm}][\text{Me}_2\text{PO}_4]$ /aqueous and aqueous media by CV measurement (vs. Ag/AgCl as a reference) was estimated to be  $-0.68$  and  $-0.66\, \text{V}$ ,

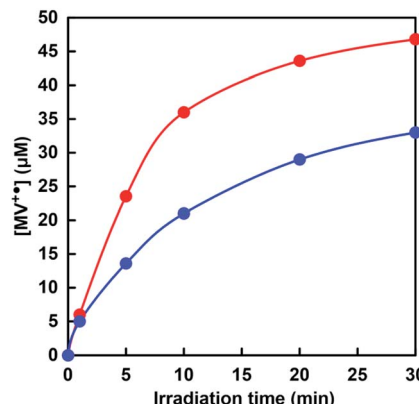


Fig. 9 Time dependence of the concentration changes of  $\text{MV}^{+*}$  in the solution consisting of TEOA, ZnTPPS and MV with visible-light irradiation. Red:  $[\text{EMIm}][\text{Me}_2\text{PO}_4]$ /water media; blue: water media.

respectively. Gibbs free energy ( $\Delta G$ ) for visible-light-driven electron transfer from the  ${}^3\text{ZnTPPS}^*$  to MV in  $[\text{EMIm}][\text{Me}_2\text{PO}_4]$ /aqueous and aqueous media was estimated using the redox potentials of  ${}^3\text{ZnTPPS}^*$  and MV. The  $\Delta G$  values for visible-light-driven of the electron transfer from the  ${}^3\text{ZnTPPS}^*$  to MV in  $[\text{EMIm}][\text{Me}_2\text{PO}_4]$ /aqueous and aqueous media were calculated to be  $-6.8$  and  $-7.7\, \text{kJ mol}^{-1}$ , respectively.

Next, let us consider the reason why MV was photoreduced more efficiently in  $[\text{EMIm}][\text{Me}_2\text{PO}_4]$ /aqueous than that in aqueous media. We have previously reported on the visible-light-driven MV reduction system of TEOA and ZnTPPS in micellar media formed by cationic, anionic and nonionic surfactants. By the addition of cationic, anionic and nonionic surfactants above the critical micelle concentration in the visible-light-driven MV reduction system of TEOA and ZnTPPS, significant MV reduction proceeded compared with that in the absence of any surfactants.<sup>51,55</sup> This indicates that a cationic surfactant micelle interface was formed between ZnTPPS and MV, and efficient charge separation between  $\text{ZnTPPS}^+$  and  $\text{MV}^{+*}$  formed with visible-light irradiation could be achieved. It was also achieved for efficient charge separation between  $\text{ZnTPPS}^+$  and  $\text{MV}^{+*}$  formed with visible-light irradiation by adding a nonionic surfactant such as Triton X-100. It has been reported that photoinduced intermolecular electron transfer and charge separation processes are affected by the viscosity of the solvent containing ionic liquid.<sup>56,57</sup> The improvement in charge separation between  $\text{ZnTPPS}^+$  and  $\text{MV}^{+*}$  formed with visible-light irradiation by adding Triton X-100 indicates that the viscosity of the reaction solvent increased. When a  $[\text{EMIm}][\text{Me}_2\text{PO}_4]$  was added to the reaction aqueous media, efficient charge separation also could be achieved by increasing viscosity of the reaction solvent.

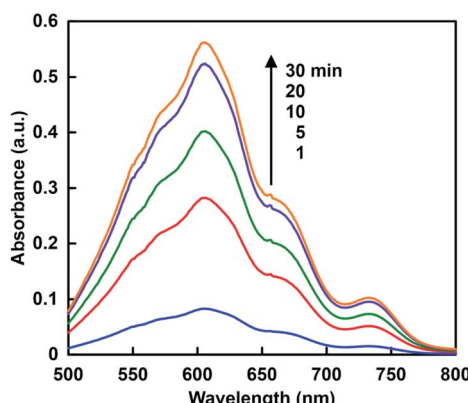


Fig. 8 Absorption difference spectra changes in the solution consisting of TEOA, ZnTPPS and MV with visible-light irradiation.

#### Visible-light-driven $\text{CO}_2$ reduction to formate with the system consisting of ZnTPPS, MV and CbFDH in the ionic liquid/aqueous media

Visible-light-driven  $\text{CO}_2$  reduction to formate was investigated by adding CbFDH to the system of MV photoreduction with



**Table 1** The turnover frequencies (TOFs) of ZnTPPS, the initial rate of  $MV^{+*}$  production ( $v_0$ ), total  $MV^{+*}$  production and yield of MV to  $MV^{+*}$  conversion in  $[EMIm][Me_2PO_4]$ /aqueous and aqueous media after 30 min irradiation

Reaction media	TOF of ZnTPPS (min <sup>-1</sup> )	$v_0$ (μM min <sup>-1</sup> )	Total $MV^{+*}$ production (μM)	Yield of MV to $MV^{+*}$ conversion
$[EMIm][Me_2PO_4]$ /aqueous media	4.7	4.7	46.8	0.47
Aqueous media	3.3	2.7	33.0	0.33

photosensitization of ZnTPPS in the presence of TEOA using  $[EMIm][Me_2PO_4]$ /aqueous media. When the reaction mixture consisting of ZnTPPS, MV, TEOA and CbFDH in  $CO_2$  saturated sodium pyrophosphate buffer containing  $[EMIm][Me_2PO_4]$  was irradiated with visible-light at 30 °C and formate production was observed with irradiation time as shown in Fig. 10 (red).

The concentration of formate production after 180 min irradiation with the system using  $[EMIm][Me_2PO_4]$ /aqueous media was estimated to be 80 μM. The experimental error was calculated as an average of three experiments. In all experiments, the error was within 5%, and the reproducibility was satisfactory. In contrast, the concentration of formate production after 180 min irradiation with the system using aqueous media was estimated to be 100 μM. Moreover, no formate production was observed under dark or in the absence of  $CO_2$  condition. The effects of the above five components, TEOA, ZnTPPS, MV and CbFDH on the  $CO_2$  reduction to formate were investigated. It was found that no formate was produced even in the missing of one of the above five components, TEOA, ZnTPPS, MV, CbFDH and  $CO_2$ . In this reaction system, in the absence of the electron donor TEOA, no reduction of MV by the photosensitization of ZnTPPS proceeded. Next, in the absence of the electron mediator MV in this reaction system,  $MV^{+*}$ , co-enzyme of CbFDH, is not produced by irradiation, so that no CbFDH-catalyzed  $CO_2$  reduction proceeded. In addition, we attempted visible-light-driven  $CO_2$  reduction with TEOA and ZnTPPS in the absence of CbFDH, but no formate production was observed. These results were obtained in both  $[EMIm]$

$[Me_2PO_4]$ /aqueous and aqueous media. In this reaction system, no CbFDH-catalyzed  $CO_2$  reduction to formate proceeded unless  $MV^{+*}$ , co-enzyme of CbFDH, was produced by irradiation in  $[EMIm][Me_2PO_4]$ /aqueous and aqueous media. When the solution consisting of TEOA, ZnTPPS, NAD<sup>+</sup> and CbFDH in  $CO_2$  saturated  $[EMIm][Me_2PO_4]$ /aqueous media was irradiated, moreover, no formate was produced with the increase in irradiation time. As no NADH was produced with the visible-light sensitization of ZnTPPS,  $CO_2$  reduction with CbFDH did not proceed in  $[EMIm][Me_2PO_4]$ /aqueous media or aqueous media. Since it is predicted that  $CO_2$  is captured and dissolved in the reaction media by using a cationic ionic liquid,  $[EMIm][Me_2PO_4]$ , the relationship between the amount of  $CO_2$  in the reaction media and CbFDH-catalyzed formate production will be investigated in the future.

The rate for visible-light-driven  $CO_2$  reduction was determined from the concentration of formate production in  $[EMIm][Me_2PO_4]$ /aqueous and aqueous media within 1 h irradiation and were estimated to be 45 and 60  $\mu\text{mol h}^{-1}$ , respectively. The turnover frequency of ZnTPPS in the system of visible-light-driven  $CO_2$  reduction to formate with CbFDH and MV in  $[EMIm][Me_2PO_4]$ /aqueous and aqueous media was estimated to be 4.5 and 6.0  $\text{h}^{-1}$ , respectively. Therefore, the ZnTPPS appeared to serve as the system for transferring electrons from TEOA to a more reductive molecule using MV in  $[EMIm][Me_2PO_4]$ /aqueous and aqueous media. Moreover, the turnover frequency of MV in  $[EMIm][Me_2PO_4]$ /aqueous and aqueous media were estimated to be 0.45 and 0.60  $\text{h}^{-1}$ , respectively. The turnover frequency of CbFDH in the system using  $[EMIm][Me_2PO_4]$ /aqueous and aqueous media were estimated to be 4.9 and 6.5  $\text{h}^{-1}$ , respectively. The turnover frequencies of ZnTPPS, MV and CbFDH, and total formate production in  $[EMIm][Me_2PO_4]$ /aqueous and aqueous media after 180 min irradiation with this system were summarized in Table 2.

As mentioned in the previous section, the CbFDH-catalyzed oxidation of formate to  $CO_2$  and reduction of  $CO_2$  to formate was slower in the  $[EMIm][Me_2PO_4]$ /aqueous media than in the aqueous media. However, in the visible-light-driven  $CO_2$  reduction system of ZnTPPS, MV and CbFDH with  $[EMIm][Me_2PO_4]$ /aqueous media, the formate production concentration after 180 min decreased by only 20% as compared with the system in aqueous media. One of the reasons for this is that the photoreduction of MV by ZnTPPS in  $[EMIm][Me_2PO_4]$ /aqueous media proceeds more efficiently than in the aqueous media system. Since the catalytic activity of CbFDH did not decrease significantly even in  $[EMIm][Me_2PO_4]$ /aqueous media, it can be expected that various visible-light-driven  $CO_2$  reduction of ZnTPPS, MV and CbFDH in the various ionic liquid can be constructed in the future.

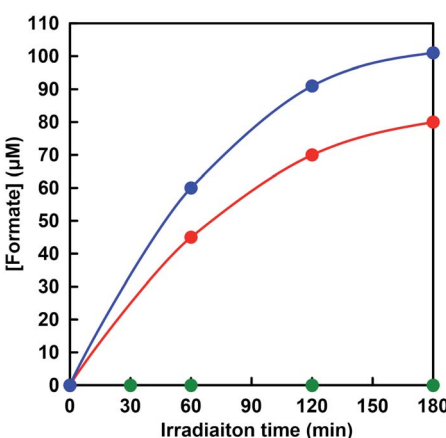


**Fig. 10** Time dependence of the concentration of formate changes in the solution consisting of TEOA, ZnTPPS, MV and CbFDH with visible-light irradiation. Red:  $[EMIm][Me_2PO_4]$ /water media; blue: water media. Green: under dark condition.



**Table 2** The turnover frequencies (TOFs) of ZnTPPS, MV and CbFDH, and total formate production after 180 min with visible-light-driven  $\text{CO}_2$  reduction to formate with CbFDH and ZnTPPS in [EMIm][Me<sub>2</sub>PO<sub>4</sub>]/aqueous and aqueous media

Reaction media	TOF of ZnTPPS (h <sup>-1</sup> )	TOF of MV (h <sup>-1</sup> )	TOF of CbFDH (h <sup>-1</sup> )	Total formate production ( $\mu\text{M}$ )
[EMIm][Me <sub>2</sub> PO <sub>4</sub> ]/aqueous media	4.5	0.45	4.9	80
Aqueous media	6.0	0.60	6.5	100

## Conclusions

In this work, to enable the development of the visible-light-driven  $\text{CO}_2$  reduction to formate with the system of a photosensitizer and CbFDH in ionic liquid/aqueous media, CbFDH-catalyzed formate oxidation and  $\text{CO}_2$  reduction are investigated in ionic liquid, [EMIm][Me<sub>2</sub>PO<sub>4</sub>] and aqueous media. The catalytic activity of CbFDH for formate oxidation and  $\text{CO}_2$  reduction did not decrease significantly even in [EMIm][Me<sub>2</sub>PO<sub>4</sub>]/aqueous media, compared with that in aqueous media. The visible-light-driven reduction of MV by ZnTPPS in [EMIm][Me<sub>2</sub>PO<sub>4</sub>]/aqueous media proceeds more efficiently than in the aqueous media system. In the visible-light-driven  $\text{CO}_2$  reduction to formate system of ZnTPPS, moreover, MV and CbFDH with [EMIm][Me<sub>2</sub>PO<sub>4</sub>]/aqueous media, the formate production concentration after 180 min decreased by only 20% as compared with the system in aqueous media. The melting point of [EMIm][Me<sub>2</sub>PO<sub>4</sub>] used in this study is estimated to be 19–21 °C, and the construction of visible-light-driven  $\text{CO}_2$  reduction to formate system near the freezing point of water has not yet been completed. In the future, we plan to construct visible-light-driven  $\text{CO}_2$  reduction to formate system in an ionic liquid with a melting point of 0 °C or less. In the future, it can be expected that the visible-light-driven  $\text{CO}_2$  reduction to formate system of ZnTPPS, MV and CbFDH can be constructed between extreme environments such as extremely low temperature and low pressure using various ionic liquids.

## Conflicts of interest

There are no conflicts to declare.

## Acknowledgements

This work was partially supported by Grant-in-Aid for Scientific Research on Innovative Areas “Artificial Photosynthesis (2406)”, “Innovations for Light-Energy Conversion (4906)”, fund for the Promotion of Joint International Research (Fostering Joint International Research (B)) (19KK0144) and Osaka City University Strategic Research Grant 2020 for top priority researches.

## Notes and references

<sup>1</sup> Smart  $\text{CO}_2$  Transformation (SCOT) project in EU Seventh Framework Program; <http://scotproject.org>.

- 2 H. Choe, J. C. Joo, D. H. Cho, M. H. Kim, S. H. Lee, K. D. Jung and Y. H. Kim, Efficient  $\text{CO}_2$ -reducing activity of NAD-dependent formate dehydrogenase from *Thiobacillus* sp. KNK65MA for formate production from  $\text{CO}_2$  gas, *PLoS One*, 2014, **9**(7), e103111.
- 3 W. S. Choi, S.-H. Lee, J.-W. Ko and C.-B. Park, Human urine-fueled light-driven NADH regeneration for redox biocatalysis, *ChemSusChem*, 2016, **9**(13), 1559–1564.
- 4 S. K. Kuk, R. K. Singh, D. H. Nam, R. Singh, J.-K. Lee and C.-B. Park, Photoelectrochemical reduction of carbon dioxide to methanol through a highly efficient enzyme cascade, *Angew. Chem.*, 2017, **129**(14), 3885–3890.
- 5 D. Mandler and I. Willner, Photochemical fixation of carbon dioxide: enzymic photosynthesis of malic, aspartic, isocitric, and formic acids in artificial media, *J. Chem. Soc., Perkin Trans.*, 1988, **2**, 997–1003.
- 6 I. Willner and D. Mandler, Characterization of palladium-.beta.-cyclodextrin colloids as catalysts in the photosensitized reduction of bicarbonate to formate, *J. Am. Chem. Soc.*, 1989, **111**(4), 1330–1336.
- 7 I. Willner, N. Lapidot, A. Riklin, R. Kasher, E. Zahavy and E. Katz, Electron-transfer communication in glutathione reductase assemblies: Electrocatalytic, photocatalytic, and catalytic systems for the reduction of oxidized glutathione, *J. Am. Chem. Soc.*, 1994, **116**(4), 1428–1441.
- 8 I. Willner and N. Lapidot, Electron-transfer communication between a redox polymer matrix and an immobilized enzyme: activity of nitrate reductase in a viologen-acrylamide copolymer, *J. Am. Chem. Soc.*, 1990, **112**(17), 6438–6439.
- 9 M. Kodaka and Y. Kubota, Effect of structures of bipyridinium salts on redox potential and its application to  $\text{CO}_2$  fixation, *J. Chem. Soc., Perkin Trans.*, 1999, **2**, 891–894.
- 10 R. Miyatani and Y. Amao, Photochemical synthesis of formic acid from  $\text{CO}_2$  with formate dehydrogenase and water-soluble zinc porphyrin, *J. Mol. Catal. B. Enzym.*, 2004, **27**(2–3), 121–125.
- 11 Y. Amao, R. Abe and S. Shiotani, Effect of chemical structure of bipyridinium salts as electron carrier on the visible-light induced conversion of  $\text{CO}_2$  to formic acid with the system consisting of water-soluble zinc porphyrin and formate dehydrogenase, *J. Photochem. Photobiol. A. Chem.*, 2015, **313**, 149–153.
- 12 S. Ikeyama and Y. Amao, The effect of the functional ionic group of the viologen derivative on visible-light driven  $\text{CO}_2$  reduction to formic acid with the system consisting of



water-soluble zinc porphyrin and formate dehydrogenase, *Photochem. Photobiol. Sci.*, 2018, **17**(1), 60–68.

13 I. Tsujisho, M. Toyoda and Y. Amao, Photochemical and enzymatic synthesis of formic acid from  $\text{CO}_2$  with chlorophyll and dehydrogenase system, *Catal. Commun.*, 2006, **7**, 173–176.

14 T. Ishibashi, M. Higashi, S. Ikeda and Y. Amao, Photoelectrochemical  $\text{CO}_2$  reduction to formate with the sacrificial reagent free system of semiconductor photocatalysts and formate dehydrogenase, *ChemCatChem*, 2019, **11**, 6227–6235.

15 Y. Amao, Viologens for co-enzyme of biocatalysts with the function of  $\text{CO}_2$  reduction and utilization, *Chem. Letts.*, 2017, **46**(6), 780–788.

16 B. S. Jayathilake, S. Bhattacharya, N. Vaidehi and S. R. Narayanan, Efficient and selective electrochemically driven enzyme-catalyzed reduction of carbon dioxide to formate using formate dehydrogenase and an artificial cofactor, *Acc. Chem. Res.*, 2019, **52**(3), 676–685.

17 [https://www.nasa.gov/directorates/spacetech/centennial\\_challenges/co2challenge/index.html](https://www.nasa.gov/directorates/spacetech/centennial_challenges/co2challenge/index.html).

18 T. Welton, Room-temperature ionic liquids, *Chem. Rev.*, 1999, **99**(8), 2071–2084.

19 F. Endres and S. Zein El Abedin, Air and water stable ionic liquids in physical chemistry, *Phys. Chem. Chem. Phys.*, 2006, **8**(18), 2101–2116.

20 D. R. MacFarlane, J. Golding, S. Forsyth, M. Forsyth and G. B. Deacon, Low viscosity ionic liquids based on organic salts of the dicyanamide anion, *Chem. Commun.*, 2001, **16**, 1430–1431.

21 J. M. Crosthwaite, M. J. Muldoon, J. K. Dixon, J. L. Anderson and J. F. Brennecke, Phase transition and decomposition temperatures, heat capacities and viscosities of pyridinium ionic liquids, *J. Chem. Thermodyn.*, 2005, **37**(6), 559–568.

22 J. S. Wilkes and M. J. Zaworotko, Air and water stable 1-ethyl-3-methylimidazolium based ionic liquids, *Chem. Commun.*, 1992, **13**, 965–967.

23 G. W. Driver, Aqueous Brønsted-Lowry chemistry of ionic liquid ions, *ChemPhysChem*, 2015, **16**(11), 2432–2439.

24 P. Wasserscheid, Volatile times for ionic liquids, *Nature*, 2006, **439**(7078), 797.

25 J. P. Armstrong, C. Hurst, R. G. Jones, P. Licence, K. R. J. Lovelock, C. J. Satterley and I. J. Villar-Garcia, Vapourisation of ionic liquids, *Phys. Chem. Chem. Phys.*, 2007, **9**(8), 982–990.

26 J. S. Wilkes, J. A. Levisky, R. A. Wilson and C. L. Hussey, Dialkylimidazolium chloroaluminate melts: a new class of room-temperature ionic liquids for electrochemistry, spectroscopy and synthesis, *Inorg. Chem.*, 1982, **21**(3), 1263–1264.

27 D. Zhao, Z. Fei, T. J. Gelbach, R. Scopelliti and P. J. Dyson, Nitrile-functionalized pyridinium ionic liquids: synthesis, characterization, and their application in carbon-carbon coupling reactions, *J. Am. Chem. Soc.*, 2004, **126**(48), 15876–15882.

28 E. F. Borra, O. Seddiki, R. Angel, D. Eisenstein, P. Hickson, K. R. Seddon and S. P. Worden, Deposition of metal films on an ionic liquid as a basis for a lunar telescope, *Nature*, 2007, **447**(7147), 979–981.

29 P. Pinto, M. Saraiva and J. Lima, Oxidoreductase behavior in ionic liquids: a review, *Anal. Sci.*, 2008, **24**(10), 1231–1238.

30 W. Hussain, D. J. Pollard, M. Truppo and G. J. Lye, Enzymatic ketone reductions with co-factor recycling: Improved reactions with ionic liquid co-solvents, *J. Mol. Catal. B*, 2008, **55**(1–2), 19–28.

31 K. Goldberg, K. Schroer, S. Lutz and A. Liese, Biocatalytic ketone reduction—a powerful tool for the production of chiral alcohols—part I: processes with isolated enzymes, *Appl. Microbiol. Biotechnol.*, 2007, **76**(2), 237–248.

32 A. J. Walker and N. C. Bruce, Cofactor-dependent enzyme catalysis in functionalized ionic solvents, *Chem. Commun.*, 2004, 2570–2571.

33 N. Wehofsky, C. Wespe, V. Cerovsky, A. Pech, E. Hoess, R. Rudolph and F. Bordusa, Ionic liquids and proteases: A clean alliance for semisynthesis, *ChemBioChem*, 2008, **9**(9), 1493–1499.

34 N. M. MicaTlo and C. M. Soares, Protein structure and dynamics in ionic liquids. Insights from molecular dynamics simulation studies, *J. Phys. Chem. B*, 2008, **112**(9), 2566–2572.

35 T. A. Page, N. D. Kraut, P. M. Page, G. A. Baker and F. V. Bright,  $J$ -aggregation of ionic liquid solutions of meso-tetrakis(4-sulfonatophenyl)porphyrin, *J. Phys. Chem. B*, 2009, **113**(38), 12825–12830.

36 M. Moniruzzaman, N. Kamiya, K. Nakashima and M. Goto, Water-in-ionic liquid microemulsions as a new medium for enzymatic reactions, *Green Chem.*, 2008, **10**(5), 497–500.

37 M. Bekhouche, L. J. Blumand and B. Doumeche, Ionic liquid-inspired cations covalently bound to formate dehydrogenase improve its stability and activity in ionic liquids, *ChemCatChem*, 2011, **3**(5), 875–882.

38 E. D'Oronzo, F. Secundo, B. Minofar, N. Kulik, A. Pometun and V. I. Tishkov, Activation/inactivation role of ionic liquids on formate dehydrogenase from *Pseudomonas* sp. 101 and its mutated thermostable form, *ChemCatChem*, 2018, **10**(15), 3247–3259.

39 H. Slusarczyk, S. Felber, M.-R. Kula and M. Pohl, Stabilization of NAD-dependent formate dehydrogenase from *Candida boidinii* by site-directed mutagenesis of cysteine residues, *Eur. J. Biochem.*, 2000, **267**(5), 1280–1289.

40 I. Okura, Hydrogenase and its application for photoinduced hydrogen evolution, *Coord. Chem. Rev.*, 1985, **68**, 53–99.

41 I. Okura, Application of hydrogenase for photoinduced hydrogen evolution, *Biochimie*, 1986, **68**(1), 189–199.

42 Y. Amao, T. Kamachi and I. Okura, Synthesis and characterization of water soluble viologen linked zinc porphyrins, *J. Photochem. Photobiol. A: Chem.*, 1996, **98**(1–2), 59–64.

43 Y. Amao, T. Kamachi and I. Okura, Photoinduced hydrogen evolution with hydrogenase and water-soluble viologen-linked zinc porphyrins, *J. Porphyrins Phthalocyanines*, 1998, **2**(3), 201–207.



44 C. Bernofsky and S. Y. C. Wanda, Formation of reduced nicotinamide adenine dinucleotide peroxide, *J. Biol. Chem.*, 1982, **257**(12), 6809–6817.

45 K. Teramura, K. Hori, Y. Terao, Z. Huang, S. Iguchi, Z. Wang, H. Asakura, S. Hosokawa and T. Tanaka, Which is an intermediate species for photocatalytic conversion of CO<sub>2</sub> by H<sub>2</sub>O as the electron donor: CO<sub>2</sub> molecule, carbonic acid, bicarbonate, or carbonate ions?, *J. Phys. Chem. C*, 2017, **121**(16), 8711–8721.

46 E. Wilhelm, R. Battino and R. J. Wilcock, Low-pressure solubility of gases in liquid water, *Chem. Rev.*, 1977, **77**(2), 219–262.

47 L. N. Plummer and E. Busenberg, The solubilities of calcite, aragonite and vaterite in CO<sub>2</sub>-H<sub>2</sub>O solutions between 0 and 90°C, and an evaluation of the aqueous model for the system CaCO<sub>3</sub>-CO<sub>2</sub>-H<sub>2</sub>O, *Geochim. Cosmochim. Acta*, 1982, **46**(6), 1011–1040.

48 T. Watanabe and K. Honda, Measurement of the extinction coefficient of the methyl viologen cation radical and the efficiency of its formation by semiconductor photocatalysis, *J. Phys. Chem.*, 1982, **86**(14), 2617–2619.

49 Y. Amao, Photoredox systems with biocatalysts for CO<sub>2</sub> utilization, *Sustainable Energy Fuels*, 2018, **2**(9), 1928–1950.

50 Y. Amao, Formate dehydrogenase for CO<sub>2</sub> utilization and its application, *J. CO<sub>2</sub> Util.*, 2018, **26**, 623–641.

51 Y. Amao and I. Okura, Effective photoinduced hydrogen evolution with hydrogenase in surfactant micelles, *J. Mol. Catal. A. Chem.*, 1996, **105**(3), 125–130.

52 S. Karastogianni and S. Girosi, *Sensing in Electroanalysis*, K. Kalcher, R. Metelka, I. Švancara and K. Vytřas, University Press Centre, Pardubice, Czech Republic, 2013/2014, Vol. 8, pp. 241–252.

53 K. Kalyanasundaram and M. Nerman-Spallart, Photophysical and redox properties of water-soluble porphyrins in aqueous media, *J. Phys. Chem.*, 1982, **86**(26), 5163–5169.

54 J. M. Lehn and J. P. Sauvage, Chemical storage of light energy. Catalytic generation of hydrogen by visible light or sunlight. Irradiation of neutral aqueous solutions, *Nouv. J. Chim.*, 1977, **1**(6), 449–451.

55 Y. Amao and I. Okura, Effect of cationic surfactant on photoinduced hydrogen evolution with hydrogenase, *J. Mol. Catal. A. Chem.*, 1995, **103**(2), 69–71.

56 R. C. Vieira and D. E. Falvey, Solvent-mediated photoinduced electron transfer in a pyridinium ionic liquid, *J. Am. Chem. Soc.*, 2008, **130**(5), 1552–1553.

57 B. Wu, M. Maroncelli and E. W. Castner Jr, Photoinduced bimolecular electron transfer in ionic liquids, *J. Am. Chem. Soc.*, 2017, **139**(41), 14568–14585.

